

Technical Notes

TECHNICAL NOTES are short manuscripts describing new developments or important results of a preliminary nature. These Notes cannot exceed 6 manuscript pages and 3 figures; a page of text may be substituted for a figure and vice versa. After informal review by the editors, they may be published within a few months of the date of receipt. Style requirements are the same as for regular contributions (see inside back cover).

Prediction of Ignition Transients in Solid Rocket Motors Employing Canted Pyrogen Igniters

C. Jasper Lal,* V. Santha,*
and

M. S. Padmanabhan†

Vikram Sarabhai Space Centre, Trivandrum, India

Introduction

LARGE solid propellant rocket motors (SPRMs) generally use head-end pyrogen igniters. Such igniters may be either of the axial-sonic type or the canted-impingement type. The axial-sonic type of igniter has a single nozzle orifice, with the igniter jet oriented along the SPRM axis. In the case of canted-impingement-type igniters the nozzle orifices are distributed circumferentially and oriented in such a way that the jets directly impinge on the propellant, leading to intense heat transfer in the impingement zone. Whatever type of igniter is employed, knowledge of the ignition transients is necessary for evolving an optimized efficient, and safe igniter.

A number of techniques have been developed for predicting the ignition transients of SPRMs. Among these, the one developed by Peretz et al.,¹ and, subsequently, further advanced by Caveny and Kuo² and later Caveny³ is the most comprehensive method. Most of the complex phenomena that occur during the induction, flame-spreading, and chamberfilling phases are taken into account in their model. However, their work considered only the axial-type, head-end pyrogen igniters.

In the present work, an analysis is developed to predict the ignition transients in SPRMs that employ canted impingement-type igniters. The analysis utilizes the essential features of the method of Peretz et al.,¹ but extends it to a wider class of igniters, as previously stated. The modification involves suitable treatment of the different regions of heat transfer arising due to pyrogen-igniter jet impingement, as described in the following.

Analysis

For the purpose of analysis, the domain is divided into three separate regions: the impingement region, the head-end region, and the downstream region (Fig. 1). The region down-

stream of the igniter-jet impingement, which is the major portion lengthwise, is analyzed by solving the one-dimensional unsteady mass, momentum, and energy conservation equations using the method of Peretz. Possible nozzle conditions of choked/unchoked flow or closure diaphragm are taken into account at the right boundary. The impingement and the head-end regions are coupled to the downstream region through its left boundary. The mass flux input to the downstream region through the left boundary is calculated as the sum of the computed mass fluxes generated at the propellant surface in the mass flux. The latter is taken as an input from the igniter nozzle geometry and the measured pressure history in the igniter during separate igniter static tests. To determine the propellant mass flux generated in the impingement region the area of igniter jet impingement is to be calculated first. This is done using the data of Lover⁴ for different conditions of jet exit-to-ambient pressure ratios and exit Mach numbers. From the calculated jet boundary, the area of impingement on the motor propellant surface is calculated for the given igniter geometry and orientation. The impingement heat transfer is calculated using the expression developed by Martin⁵ for the heat transfer between impingement gas jets and solid surfaces:

$$\frac{Nu}{Pr^{0.42}} = \frac{D}{r} \frac{1 - 1.1(D/r)}{1 + 0.1\left(\frac{H}{D} - 6\right)\frac{D}{r}} F(Re)$$

with

$$F(Re) = 2Re^{1/2} \left[1 + \frac{Re^{0.55}}{200} \right]^{0.5}$$

where H is the distance from the igniter exit to the point of impingement, Re is the Reynolds number based on the jet exit diameter, D is the jet exit diameter, and r is the radial distance. In the head-end region, radiation is assumed to be the dominant mode of heat transfer. Under the computed heat flux conditions in the respective regions, propellant heat-up to igni-

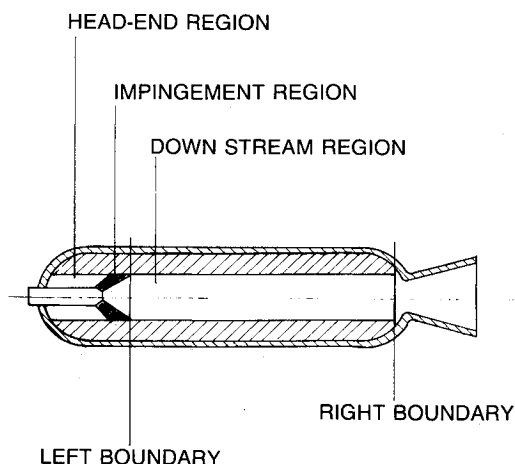


Fig. 1 Schematic of igniter with different regions of analysis.

Received March 23, 1987; revision received May 2, 1988. Copyright © 1988 American Institute of Aeronautics and Astronautics, Inc. All rights reserved.

*Scientist/Engineer, Heat Transfer and Combustion Research Division.

†Head, Combustion Section, Heat Transfer and Combustion Research Division.

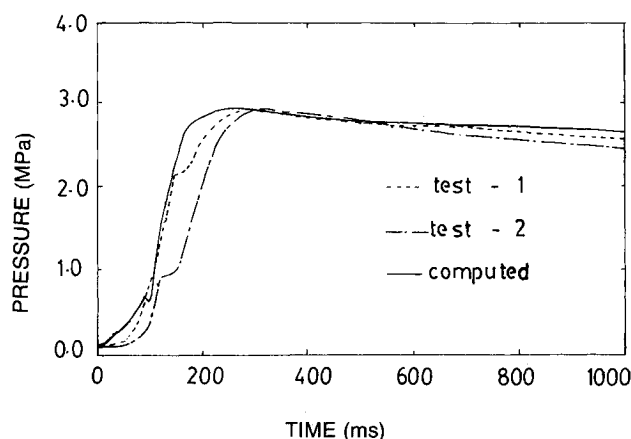


Fig. 2 Comparison of computed and measured pressure transients.

tion is computed by solving a one-dimensional heat conduction equation in the propellant. Critical ignition temperature criterion is applied to determine the point of ignition. Following ignition in the impingement and head-end regions, the mass flux generated from the propellant surface in these regions is calculated at every instant from the known burning rate law of the propellant. Based on the mass fractions of the igniter products and the generated gases at the motor propellant, the effective specific heat and temperature of the resultant mixture is calculated and is input at the left boundary for the downstream region.

Results

Computations have been performed using the method and the results compared with available test data. The test motor has a 8.6 m monolithic grain of AP-PBAN-A1 propellant system. The port is a six-pointed star configuration. The motor employs a canted-impingement-type pyrogen igniter with a cant angle of 45 deg. The impingement area amounts to 6% and the head-end area to 12% of the total initially exposed propellant burning surface area. The downstream region constitutes 87% of the grain length. A nozzle diaphragm, designed to burst at 0.6 MPa, is provided. Figure 2 compares the measured and computed pressure transients at the motor head end. The computations show a more rapid pressure drop upon nozzle diaphragm burst; this may be a consequence of assuming instantaneous diaphragm burst resulting in immediate availability of the full throat area for exhaust of combustion products, whereas the actual mechanical system may involve a small but finite time delay of a few milliseconds. The computed rate of pressurization is seen to be higher than the test values. This may be due to the limitation of the one-dimensional flow analysis, which implies instantaneous circumferential flame spread. The prediction procedure may be improved by a two-dimensional flow analysis.

References

- ¹Peretz, A., "The starting Transient of Solid Propellant Rocket Motors with High Internal Gas Velocities," Aerospace and Mechanical Sciences Report No. 1100, Princeton University, Princeton, NJ, April 1973.
- ²Caveny, L. H. and Kuo, K. K., "Ignition Transients of Large Segmented Rocket Boosters," NASA CR-150162, April 1976.
- ³Caveny, L. H., "Extensions to Analysis of Ignition Transients of Segmented Rocket Motors," NASA CR-150632, Jan. 1978.
- ⁴Love, E. S., "Experimental and Theoretical Studies of Axisymmetric Free Jets," NASA TR-R-6, 1959.
- ⁵Martin, H., "Heat and Mass Transfer Between Impinging Gas, Jets and Solid Surfaces," *Advances in Heat Transfer*, Vol. 13, 1977.

Cesium Density Measurements with a Laser Diode in a Magnetohydrodynamic Generator

E. M. van Veldhuizen*
Eindhoven University of Technology,
Eindhoven, the Netherlands

I. Introduction

THE development of magnetohydrodynamic (MHD) generators as a topping cycle in electrical power plants involves many aspects. Plasmaphysics, gasdynamics, and power electronics are the main topics. The work performed at the Eindhoven University of Technology is concentrated on the generator itself. Therefore, as many measurements as possible are carried out to obtain data of the plasma inside the channel.

In this Note, the cesium density measurement is described in detail. Other diagnostics are discussed elsewhere.¹ In the closed-cycle blowdown generator as used in our laboratory cesium is added to the argon gas to enhance conductivity. The amount of cesium can be adjusted as a weight fraction of the argon. The distribution of cesium in the generator, however, is unknown. By means of line absorption the density inside the generator can be measured, i.e., the ground state density of an atom is measured by the absorption of a resonance line. In the case of cesium there are two options: 894.4 and 852.1 nm, i.e., the near infrared. The lineshapes of these transitions are strongly influenced by collisions with the argon atoms. Accurate experimental data for the argon-cesium case are available.² The best signal-to-noise ratio is obtained from the experiment with a wavelength of 854.6 nm, i.e., 2.5 nm in the red wing of the 852.1-nm cesium line, as is pointed out in Ref. 1.

This wavelength is close to the wavelength of the GaAlAs laser diode. Since the wavelength of these lasers depends strongly on the temperature, some of them have a built-in Peltier element for temperature stabilization. This element can also be used to tune the wavelength within a region of several nanometers, thus obtaining the desired wavelength for the absorption measurement.

II. Laser Stabilization

The laser used here is a TXSK 3501 made by AEG-Telefunken with a nominal wavelength of 850 nm and a maximum output power of 10 mW at a current of 150 mA. Built in are a Peltier element, an NTC resistor, and a monitor diode. The laser is multimode. Its mode spacing is approximately 0.25 nm, and 10–20 modes are present depending on the output power. The wavelength is selected with a 1-m Jobin-Yvon monochromator, and the intensity is measured with a photomultiplier with a GaAs cathode (Hamamatsu R636). Using a slit width of 0.1 mm, this monochromator selects the wanted mode. A disadvantage could be that 90% of the output power of the laser is not used, but for this experiment the remaining 10% is satisfactory.

When the laser is cooled with the Peltier element the wavelength shifts toward the red. The wavelength of maximum power can thus be tuned from 838 to 862 nm, according to the

Received April 1, 1988; revision received Jan. 1, 1989. Copyright © American Institute of Aeronautics and Astronautics, Inc. All rights reserved.

*Member of the Scientific Staff, Electrical Energy Systems Division, Department of Electrical Engineering.